

Aerodynamic Characteristics of an Unsteady Separated Flow

M. S. Francis,* J. E. Keesee,† J. D. Lang,‡ G. W. Sparks Jr.,§ and G. E. Sisson¶
U.S. Air Force Academy, Colo.

The results of experiments in which an unsteady separating flow was generated on the surface of an airfoil immersed in a subsonic wind-tunnel freestream are discussed. An investigation of the global ensemble averaged vorticity field generated by oscillation of a fence-type spoiler located on one surface of the airfoil has confirmed the presence of a dynamically evolving vortex-like structure bearing a strong resemblance to the one encountered in classical dynamic stall. The growth and development of the shear layer region is characterized through isovorticity contour maps at select phase points during the motion cycle. A detailed description of flowfield behavior is provided for several values of the dimensionless spoiler frequency and freestream Reynolds number. The correlation of these results with corresponding surface pressure measurements is also presented.

Nomenclature

- c = airfoil chord length
 C_p = pressure coefficient based on freestream dynamic pressure, $(p - p_\infty) / \frac{1}{2} \rho U_\infty^2$
 h_s = instantaneous spoiler height, maximum value given by h_{smax}
 k = dimensionless frequency based on airfoil semichord, $\omega c / 2U_\infty$
 Re = Reynolds number based on freestream velocity, $U_\infty c / \nu$
 U_c = characteristic growth velocity of the separated region in the freestream direction
 U_∞ = freestream velocity
 Γ = circulation around a closed contour, C
 α = X -configuration hot-film probe crossflow angle
 ξ = vorticity vector, $\xi = \xi_x \hat{i} + \xi_y \hat{j} + \xi_z \hat{k}$ (a prime denotes dimensionless form)
 ϕ = spoiler oscillation phase angle, $\phi = \omega t$
 ω = spoiler oscillation frequency, rad/s
 $\langle \rangle$ = spatial average

Introduction

DURING flight vehicle maneuvers at high angles of attack, dynamic stall or other complex phenomena involving time-varying flow separation may occur resulting in aerodynamic loads that differ significantly from those predicted from steady flow considerations. Future designs of advanced maneuverable flight vehicles may well seek to incorporate the advantageous effects of these highly energetic flows in a positive way to enlarge the effective flight envelope. The capability to stabilize and control flow behavior necessary for productive improvements in performance must

be preceded by a more complete knowledge of the mechanics of unsteady separation.

Problems associated with various forms of unsteady separation have been recognized and studied for some time, ranging from shock wave boundary-layer interactions encountered in high-speed flight^{1,2} to the understanding of lift generation mechanisms for various forms of insect life.³ A phenomenon of recent interest exhibiting global unsteady separation characteristics due to the pitching motion of an airfoil is that of dynamic stall.^{4,9} A comprehensive review of progress on many of the problems involving unsteady separation can be obtained from recent articles by McCroskey.^{10,11}

The investigation discussed below is directed toward a realistic characterization of these types of flows through an improved understanding of the role of the dominant physical mechanisms. To satisfy the need for a controlled form of unsteady separation exhibiting a simplified two-dimensional flow geometry, an experiment was devised employing an airfoil with an oscillating fence-type spoiler located at mid-chord on one surface immersed in a subsonic wind-tunnel freestream. With a capability to adjust spoiler geometry parameters, oscillation amplitude and frequency characteristics, and mean flow Reynolds number, this configuration provided for control of the size of the separated region while fixing the separation point with respect to the freestream coordinate direction. An additional advantage of this configuration was the extensive data base available from previous investigations of flows with similar geometric characteristics.¹²⁻¹⁵

Previous research by the authors^{16,17} using a configuration similar to that employed here has resulted in the development of a semi-empirical model of unsteady separation verified with surface pressure field measurements exclusively. Experimental results confirmed the existence of both a lag in the growth of the separated region and an overshoot in the steady flow pressure which were the model's essential features. The most questionable aspect involved in the extension of the model beyond its assumed limits, i.e., small perturbations and high-aspect ratio separated region geometry, was the accuracy of the flowfield description itself. The model was predicated on the concept of a growing and shrinking "bubble-like" structure, which has not been verified in the case of large, high-frequency perturbations as in some of the experiments described later.

The vortex-like structure shown to exist for the dynamic stall separation zone⁸ suggests that a logical variable to characterize this type of flow might be that of vorticity. For a two-dimensional flow, the assessment of the distribution of the mean vorticity component orthogonal to the plane of flow would provide a scalar field representation capable of

Presented as Paper 79-0283 at the AIAA 17th Aerospace Sciences Meeting, New Orleans, La., Jan. 15-17, 1979; submitted Feb. 8, 1979; revision received July 10, 1979. This paper is declared a work of the U.S. Government and therefore is in the public domain. Reprints of this article may be ordered from AIAA Special Publications, 1290 Avenue of the Americas, New York, N.Y. 10019. Order by Article No. at top of page. Member price \$2.00 each, nonmember, \$3.00 each. **Remittance must accompany order.**

Index categories: Nonsteady Aerodynamics; Viscous Nonboundary-Layer Flows.

*Chief, Mechanics Division, Frank J. Seiler Research Lab. Member AIAA.

†Research Associate, Frank J. Seiler Research Lab. Member AIAA.

‡Associate Professor of Aeronautics, Dept. of Aeronautics. Member AIAA.

§Assistant Professor of Aeronautics, Dept. of Aeronautics. Member AIAA.

¶Instructor of Aeronautics, Dept. of Aeronautics. Member AIAA.

describing the "average" motion. Since the flow is unsteady, streamlines cannot be used to provide a meaningful description of flow behavior. The use of the vorticity field description, however, does provide a method of reconstructing the velocity field, if desired. In addition, it identifies those regions where real fluid effects, e.g., viscosity, are most dominant.

The objectives of the current experiment are to describe the behavior of the outer regions of the flowfield, that is, the outer shear layer, and to correlate significant events in this part of the flowfield with the development of the surface pressure field adjacent to the separation zone. Among the parameters varied in the present study are the freestream Reynolds number and the dimensionless frequency. This investigation of the global, ensemble-averaged vorticity field resulting from simple harmonic spoiler oscillations will show that the separation zone is not merely a growing and shrinking "bubble" as previously conceptualized, but a dynamically evolving vortex-like structure bearing a strong resemblance to the one encountered in the dynamic stall flowfield.

Description of the Experiment

A NACA 0012 airfoil model having a 25.4 cm (10 in.) chord with an oscillating fence-type spoiler protruding from one surface at midchord was constructed and installed in the USAF Academy's 0.61×0.91 m (2×3 ft) subsonic wind tunnel. The model spanned the tunnel across the shorter dimension. The spoiler was constructed from 0.32-cm (0.125-in.) thick aluminum sheet material to provide sufficient rigidity during excursions through the teflon-lined groove in the airfoil surface. Movable plexiglass endplates were constructed to provide a capability to vary the aspect ratio of that portion of the airfoil over which the measurements were made. In the present experiment, these endplates were fixed at a distance of 35.6 cm (14 in.) apart, providing an aspect ratio of 1.4. The purpose of the endplates was to suppress the development of three-dimensional effects in the separated region, e.g., net axial flow in the vortex center.

The spoiler oscillation mechanism was designed using a dc motor drive to generate sinusoidal oscillations of the spoiler. The experiment was devised so that both mean height and spoiler amplitude could be adjusted to desired values. For the measurements described below, they were fixed so that the minimum height coincided with the airfoil surface while the maximum height (h_{smax}) was fixed at 1.27 cm (0.5 in.). The

spoiler motion could then be described as

$$h_s(t) = (h_{smax}/2)(1 - \cos \omega t) \quad (1)$$

The maximum fractional perturbation to the flow, expressed as a ratio of spoiler height to wing semichord, was equal to 0.1. Oscillation frequencies could be varied between 0 and 24 Hz to within 0.1 Hz resolution. This corresponds to a reduced frequency range extending from $0.0 \leq k < 1.2$, depending on the flow velocity.

All measurements were made with an airfoil angle of attack of 0 deg. This provided a suitably thin boundary layer over the surface upstream of the spoiler, thereby minimizing any interaction with the separation zone downstream of the spoiler. The freestream velocity was varied from approximately 12.2 to 41.1 m/s (40 to 135 ft/s) resulting in a Reynolds number range of $164,000 < Re < 554,000$.

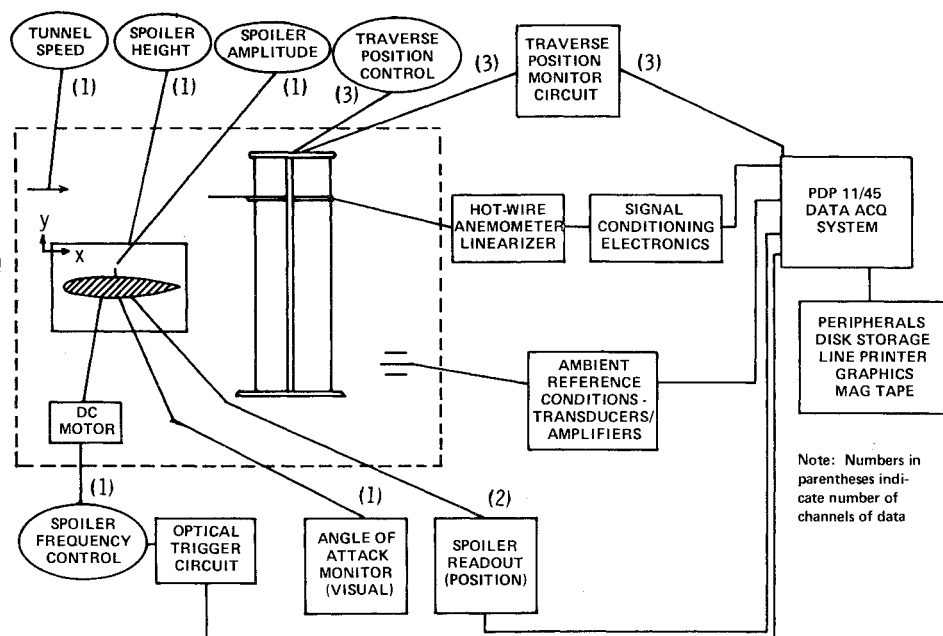
An overall schematic of the experimental apparatus is provided in Fig. 1. The airfoil model was instrumented with 16 precision miniature pressure transducers located chordwise along its centerline. Six of these units were located aft of the spoiler on the airfoil upper surface. A multicomponent, constant temperature, linearized hot-film anemometry system was employed for velocity field measurements in the outer shear layer region of the separation zone. Additional details related to the design and operation of the instrumentation can be found in Ref. 18.

Experimental Method

Averaging Technique

The present method of flowfield characterization makes use of the time-varying mean value of the surface pressure and vorticity field variables to describe the flow. The method of extracting this quantity involves the generation of a phase-locked, ensemble average of the variable being examined. The signal characterizing the variable is synchronized to a repeatable event (a predetermined spoiler position) and then sampled with resultant records stored in the digital computer. Using a prescribed number of these records, each triggered at the same phase point, data at common phase points were combined to form an ensemble average for that value of the phase. Resultant averages from all phase points were then recombined to provide the average time history of the variable for that spatial location. Mean square values and other

Fig. 1 Schematic of experimental apparatus.



combinations of the variables were obtained with an ensemble averaging technique similar to that used for the mean flow data. A 25-record average was selected for use in all measurements reported here.

Vorticity Measurement Technique

The vorticity field was inferred from velocity field measurements using a technique described previously by Francis et al.¹⁹ and extended to unsteady flows by Keese et al.¹⁸ The technique involves the literal application of the definition of circulation

$$\Gamma(t) = \oint_C \mathbf{U}(x, t) \cdot d\mathbf{x} \quad (2)$$

If the contour is chosen to lie in the x - y plane, for example, and A is the resulting enclosed planar area, the expression for the spatially averaged component of vorticity orthogonal to the measurement plane can be expressed as

$$\langle \xi_z(t) \rangle = \frac{1}{A} \oint_C \mathbf{U}(x, y, t) \cdot d\mathbf{x} \quad (3)$$

If a number of small contours are arranged in an aggregate, the distribution of vorticity in the enclosed region can be inferred. Since Eq. (3) is a result of kinematic conditions, the contour C may take any shape. In practice, it is convenient to choose a contour array geometry that is related to the flow being investigated or the experimental apparatus being employed. Selection of this geometry in the present case was based on a number of factors, including the probe measurement volume, the location and size of the separated region and shear layer, and the desired resolution of the vorticity field. The time-varying mean value of vorticity for the i th element of the mesh is given by

$$\langle \xi_z(t) \rangle_i = \frac{1}{A_i} \oint_{C_i} \mathbf{U}(x, t) \cdot d\mathbf{x} \quad (4)$$

The measurement grid that was used involved a total of 390 spatial sampling locations. The configuration was predicated on a knowledge of the flowfield obtained from flow visualization photographs and the limitations just discussed.

Sources of Error

The use of miniature dynamic piezoresistive transducers to assess the surface pressure distribution is straightforward and has been documented previously.¹⁷ The nature of errors incurred in the application of the vorticity measurement technique to an unsteady separated flow, however, is not immediately apparent.

The use of the hot-film anemometer presented certain limitations on the possible measurement locations due to the intermittent, reversing nature of the flow. Flow reversal was found to be the most pronounced near the airfoil surface with a low velocity region existing immediately behind the spoiler and extending downstream (Fig. 2). The use of the hot-film technique was therefore confined to the outer shear layer region and a portion of the dead air zone. To further insure that only valid data were sampled, the values of several additional variables were monitored to insure that erroneous data were not collected. Data locations where the local x component of velocity did not exceed 25% of the freestream value were annotated. In addition, a computation of the root mean square (rms) values of the u and v velocity fluctuations was obtained at select sampling locations. Analog and digital circuits were monitored continuously for overrange conditions. Values of the instantaneous X -wire crossflow angle were also computed to insure that the flow angle was maintained within the linear limits of operation ($-0.5 < \tan \alpha < +0.5$). Results from a survey of this variable

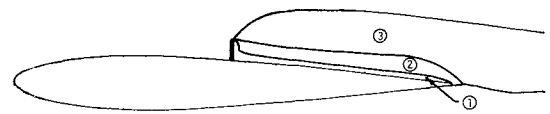


Fig. 2 General description of flow regions during unsteady separation.

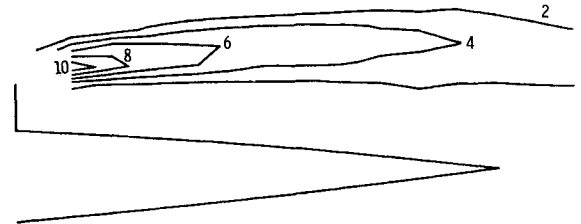


Fig. 3 Isovorticity contours associated with steady flow separation, $Re = 287,000$.

over the entire extent of the measurement array have shown that the flow angle never exceeded the linear limit of validity for more than 1.4% of the total measurement time in the worst case. A more complete discussion of the limitations of applying the X -configuration hot-film probe to this type of measurement, especially with regard to the out-of-plane velocity component error, is provided in Ref. 19.

Other sources of measurement error include probe positioning resolution, sampling accuracy, and the accuracy of the spatial integration scheme.¹⁸ A worst-case value for the total error for a typical contour employed in the present experiment has been estimated at approximately 2.5%.

Steady Flow Results

Before initiating a discussion of the effects of unsteady motion on the evolution of flow separation, it is instructive to consider the case of steady separation. The mean vorticity field associated with the shear layer behind the spoiler (which is fixed and extended to its maximum height above the surface, h_{smax}) is shown in Fig. 3. The contours are presented for appropriate nondimensionalized values of the vorticity as follows:

$$\xi'_z = \xi_z c / 2U_\infty \quad (5)$$

This variable is similar in structure to the dimensionless frequency k , giving it the same form as a Strouhal number.

The symmetry of the shear layer with respect to a line extending downstream from the tip of the spoiler is apparent. Although this figure shows the result for only a single value of the freestream Reynolds number, it is interesting to note that similar results occur over the entire range of Reynolds numbers examined in the present case. Not only are the shear layer characteristics symmetrical in these cases as well, but the contour lines representing identical values of the dimensionless vorticity are observed to almost coincide with the same spatial locations. This comparison suggests that the dimensionless vorticity expressed in the form presented above represents a similarity variable, at least in the steady flow case. Additionally, this implies that the local strength of the vorticity field is proportional to the freestream velocity. These results are also consistent with the results of previous investigators who have noted that the length of the separation "bubble" based on the reattachment point is linearly proportional to the spoiler height in the steady flow case.

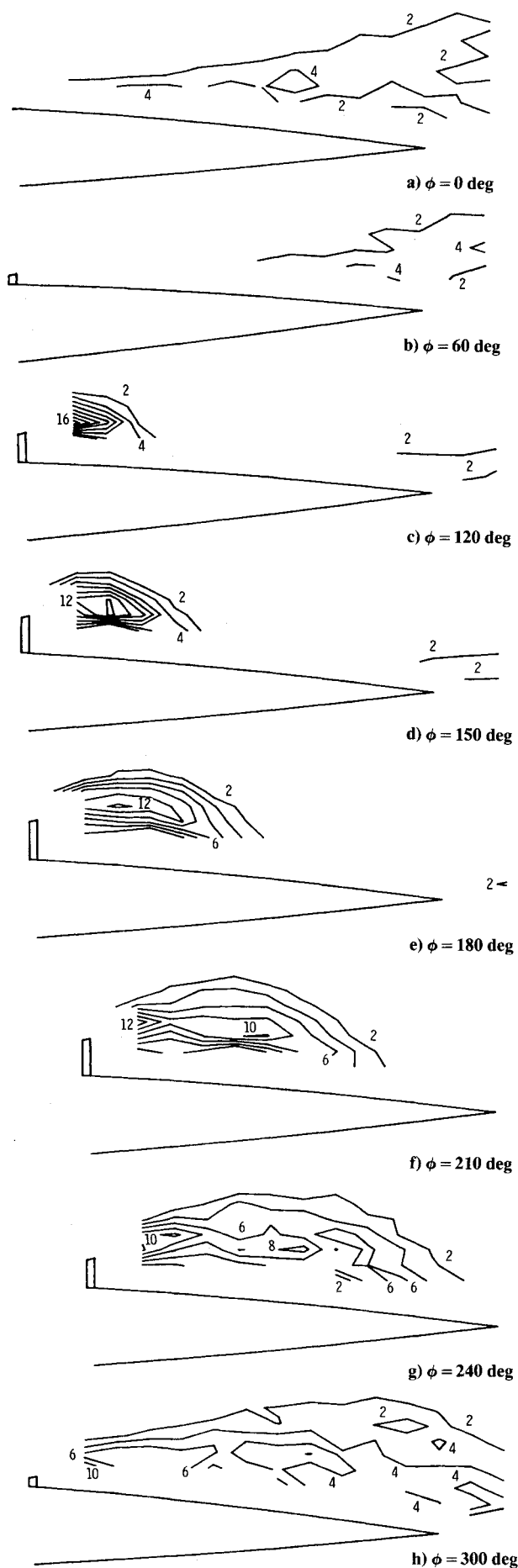


Fig. 4 Isovorticity contours associated with unsteady flow separation, $k = 1.2$, $Re = 180,000$.

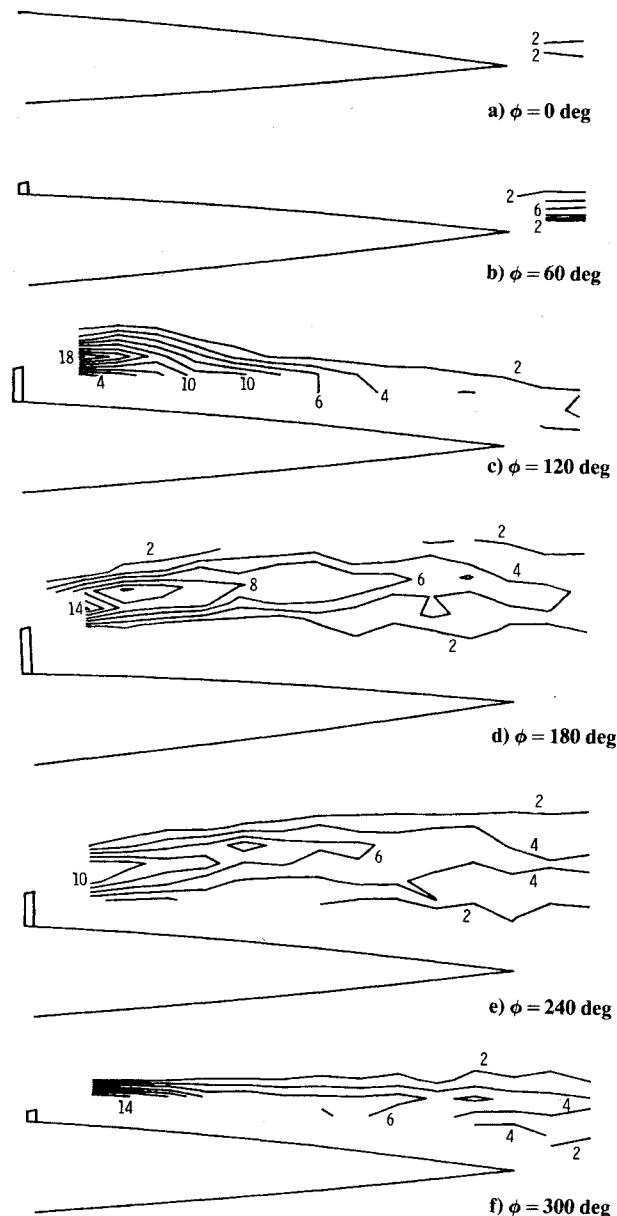


Fig. 5 Isovorticity contours associated with unsteady flow separation, $k = 0.2$, $Re = 287,000$.

Effects of Harmonic Spoiler Motion

The steady flow results discussed above can now be contrasted with the flowfield behavior evoked by unsteady spoiler oscillations. Flowfield development is displayed for an average cycle of motion for two different values of the dimensionless frequency in Figs. 4 and 5. The evolution of the unsteady separation zone is shown using isovorticity contour maps at select values of the phase angle. Only vorticity directed in the positive z direction (sense into the page) is considered in the discussion that follows. Vorticity having an opposite sense was detected near the edges of the measurement region and anticipated close to the airfoil and spoiler surfaces due to local flow reversal. It is not considered in the current study, however, due to limitations in instrumentation and measurement methods.

An examination of the upstroke portion of the cycle at high frequency (Fig. 4) reveals the formation and growth of an energetic, tightly wound vortex structure downstream of the spoiler. This interpretation is confirmed by the high level of vorticity observed and the high degree of curvature in the shear layer geometry when compared to steady flow results. A similar vortex is observed in the low-frequency example, but

with less curvature in the shear layer shape and sustained for a shorter portion of the cycle. While the growth lag described by previous investigators is apparent, the characterization of the separation zone interior as a "dead-air region" must be questioned, at least during this portion of the cycle. The higher peak vorticity magnitude observed in the unsteady cases comes as really no surprise when one considers that there are now two sources of vorticity, one being the action of the freestream as it passes over the spoiler tip, and the other related to the shearing action parallel to the oscillating spoiler face. The energetic, rotating flow is formed by a combination of the fluid motion induced by the spoiler oscillations and the entrainment tendencies of the shear layer generated by the freestream. If one attempts to compare the capability to generate vorticity by these two mechanisms through a ratio of maximum spoiler oscillation velocity to freestream velocity, the resulting parameter is expressed as

$$k' = (h_{s_{\max}}/c)k \quad (6)$$

As the value of this modified, dimensionless frequency parameter approaches unity, one expects that the capability for vorticity generation from these two mechanisms becomes comparable.

The structure of the tightly wound vortex is observed to deform significantly under the influence of the freestream during the midportion of the cycle. As the spoiler nears its maximum height, its velocity h_s decreases rapidly. The result, at the low spoiler frequencies, is that the flowfield attempts to "catch up" with the corresponding steady flow configuration (see Fig. 5). At dimensionless frequencies near unity, the downstroke portion of the cycle is observed to begin before this relaxation of the shear layer can occur. As a result, a flow configuration resembling that encountered in steady flow never really develops.

While the growth of the separated region on the spoiler upstroke might be viewed loosely as a "bubble"-like structure whose characteristic size lags a corresponding steady flow value, no such interpretation can result from an observation of the vorticity field on the spoiler downstroke. At low frequency (Fig. 5), the detached shear layer appears to retract toward the airfoil surface with the spoiler in a quasisteady manner. At higher frequencies, however, the vorticity bearing structure is observed to literally detach from the spoiler and wash off the surface through convection by the freestream (Fig. 4).

The deformation of the tightly wound vortex through entrainment by the freestream-generated shear layer prompts an inquiry regarding the conditions for which this structure might be capable of sustaining its cylindrical symmetry throughout the motion cycle. The ability of the vortex to retain its identity in this case would seem to depend somehow on the ratio of the energy of the rotational motion associated with the vortex as compared to the freestream kinetic energy. Simple dimensional arguments show that this ratio is proportional to the square of the dimensionless frequency. As the value of this ratio approaches unity, the vortex should then be able to maintain its structure, at least through its traversal over the upper surface of the airfoil. This behavior has been verified by Francis et al.²⁰ using hydrogen bubble flow visualization data obtained in a water tunnel at low Reynolds numbers. It should be emphasized that the effect of turbulence has not been accounted for in this simple argument; this also must be taken into consideration when attempting to develop a more accurate characterization of separated region development at high Reynolds numbers.

Vortex Growth Characteristics

Of particular interest in the evolution of the unsteady, separated flowfield are the detailed growth characteristics of the vortex formed behind the spoiler during the upstroke

motion. The development of the vortex geometry is of significance if one accepts the premise that vortex-related induced velocities near the surface are responsible for the significant suction levels discussed in the next section.

An examination of the microscale structure of the vortex during its inception (near the surface) was not possible due to the orientation and location of the measurement points and spatial averaging technique employed here. Initial detection of the vortex did not occur until the phase angle reached a value of approximately 40-70 deg, and when the characteristic dimensions of the structure were of the order of $h_{s_{\max}}$.

The combined decrease of maximum rotation rates with elongation and lateral expansion made it exceedingly difficult to formulate a single parameter capable of relating all facets of vortex growth. As a result, each of these characteristic traits related to vortex evolution will be dealt with individually.

The lateral extent of the outer shear layer appears to be controlled primarily by the value of the spoiler height. The longitudinal growth of the separated region, however, was found to be related primarily to the oscillation frequency. An assessment of the length of the separation zone was accomplished by tracking the motion of individual isovorticity contours in the x direction at prescribed values of the lateral (y) coordinate. Although the length parameter defined in this manner is somewhat arbitrary depending on the vorticity magnitude selected, it provides a useful method for observing the degree of nonlinearity in the growth of the separation zone. Some of these results are presented in Fig. 6 for several combinations of dimensionless frequency and Reynolds number. In this example, the movement of the aftmost portion of the contour representing a value of two was observed along the line $y/c = 0.09$ (origin at the trailing edge). Similar results for other values of the vorticity magnitude reveal a corresponding behavior of the shape and slope of the growth characteristics.

The nearly linear nature of these characteristics suggests that the growth of the vortex is directly proportional to the time of evolution (phase angle) and not correlated to the nonlinear motion of the spoiler itself, at least during the midportion of the upstroke. One observes that the higher the value of k , the more extensive the linear region. An alternative statement is that the vortex remains as an identifiable entity for a larger fraction of the period at higher frequencies.

The individual slopes of the lines shown in Fig. 6 can be used to provide the values of the characteristic longitudinal growth velocity. This variable can be formulated in a dimensionless way as:

$$\frac{U_c}{U_\infty} = A \cdot \frac{\Delta(x/c)}{\Delta\phi} \quad (7)$$

where A is an appropriate nondimensionalization factor that can be a function of the dimensionless frequency. Computed values of this parameter from experimental data show that it is not sensitive to freestream Reynolds number, at least over

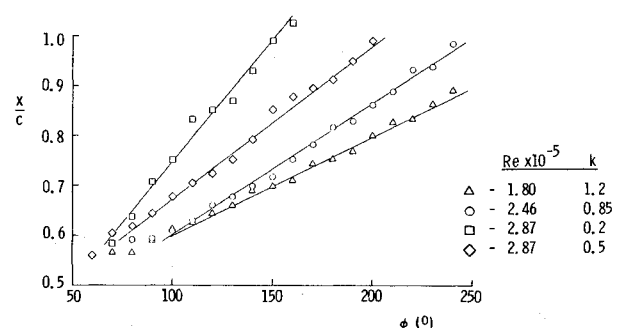


Fig. 6 Length of the separated region as a function of phase angle.

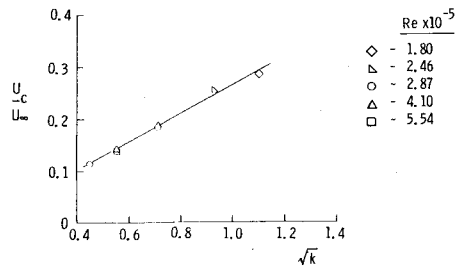


Fig. 7 Characteristic vortex growth velocity variation with dimensionless frequency.

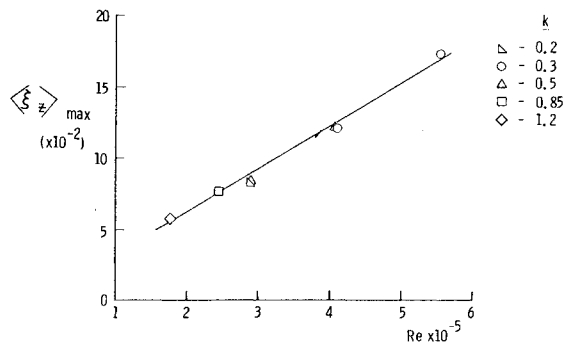


Fig. 8 Maximum value of laterally-averaged vorticity as function of Reynolds number.

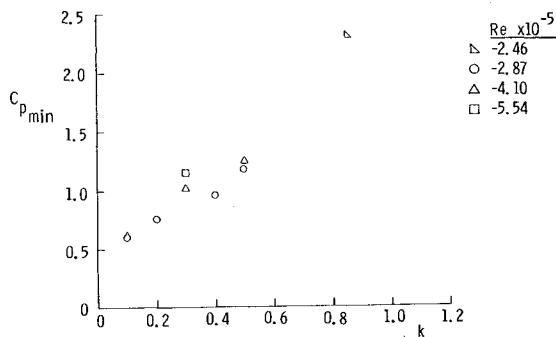


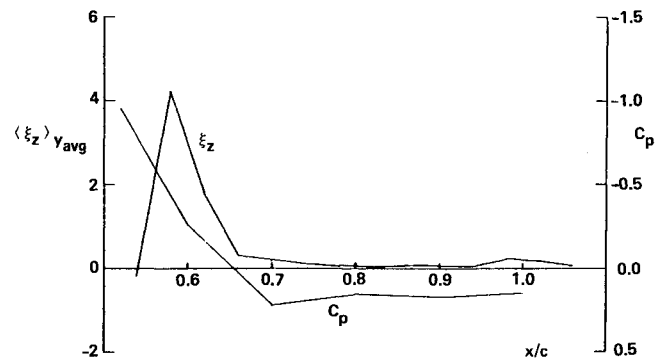
Fig. 9 Minimum pressure coefficient variation with dimensionless frequency.

the range examined. A graph of the dimensionless, convective velocity variation with the square root of the dimensionless spoiler oscillation frequency is provided in Fig. 7. The apparent linear relationship suggested by this result can be expressed as:

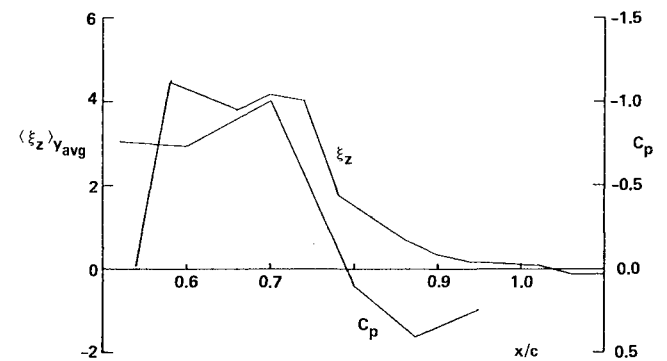
$$U_c/U_\infty = B\sqrt{k} \quad (8)$$

where B is a constant, probably related to the spoiler mean height and amplitude parameters, that equals 0.28 in the present case.

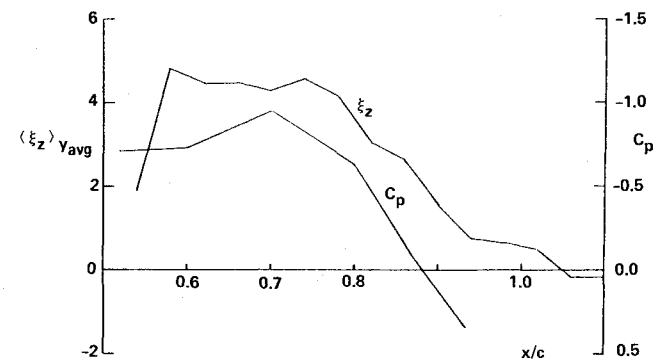
The one parameter which appears to correlate closely with Reynolds number is the maximum level of vorticity observed in the different experiments. This was observed for the steady flow examples presented earlier, but also appears true in the unsteady flow case. One must be cautious when attempting to draw conclusions from observations of ξ_{zmax} , especially because of the limited extent of the measurement grid geometry. For this reason it was felt that a more appropriate parameter might be generated by spatially averaging the vorticity in the y -coordinate direction at various stations in the downstream direction. The relationship between the maximum value of this laterally averaged variable detected during a cycle of motion and the Reynolds number is



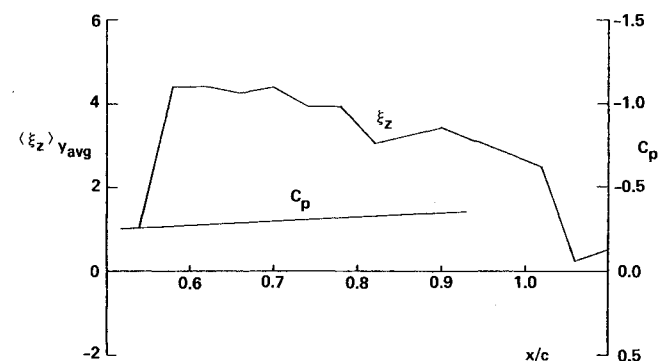
a) $\phi = 90^\circ$



b) $\phi = 150^\circ$



c) $\phi = 180^\circ$



d) $\phi = 240^\circ$

Fig. 10 Comparison of pressure distribution and laterally averaged vorticity field as function of freestream coordinate direction.

presented in Fig. 8. The linear result suggests that the peak levels of vorticity are strongly correlated to the freestream velocity and, therefore, the corresponding Reynolds number.

Correlation with Surface Pressure Field

In steady flow, an examination of the pressure coefficient downstream of a fixed spoiler protuberance indicates a

"rooftop" shape to the pressure distribution. In the case of unsteady spoiler oscillations, this distribution is modified by an increased magnitude of the suction peak, which is related to the frequency of oscillation as well as a characteristic lag in the growth of the separation zone. These results have been verified by the surface pressure data obtained in the present experiment for correlation to the vorticity field results discussed previously.

The correlation of the extent of the minimum value of the pressure coefficient with dimensionless frequency was reaffirmed and is shown in Fig. 9. The fact that this variable is more closely correlated to dimensionless frequency rather than Reynolds number suggests that it is not related to maximum vorticity levels generated within a separated region, but is instead coupled to the geometry of the separation vortex. A comparison of the isovorticity contour maps and ensemble averaged surface pressure data does, in fact, confirm this suspicion.

A convenient method for effecting a comparison between these two entities is found by employing the y -coordinate averaged vorticity distributions discussed previously. The resultant comparison is provided for several different combinations of frequency and Reynolds number in Fig. 10. The results are displayed for several select values of the phase angle.

Similarities in the separated region geometry on the upstroke are apparent. The location of the regions of maximum vorticity (indicative of the presence of the separation vortex) and the corresponding regions of local suction appear almost superimposed on one another. This correlation is especially close during the early parts of the spoiler upstroke.

As the spoiler nears its maximum extension and during the downstroke portion of the cycle, the distribution of laterally averaged vorticity is observed to nearly reach an equilibrium value. This can be explained by noting that vorticity leaving the measurement region through downstream convection is replaced by new vorticity generated at the spoiler tip (quasisteady behavior). At the same time, the pressure field is observed to flatten out in a manner reminiscent of the rooftop distribution. As the spoiler retreats, the flattened suction region is observed to decrease in magnitude while the vorticity bearing zone appears to sustain a constant level. This apparent discrepancy is simply an indicator that, during the downstroke portion of the cycle, it is not the outer shear layer behavior which dominates the local surface pressure distribution, but rather flow effects occurring closer to the airfoil surface.

Concentrating on that part of the cycle during which the energetic vortex is formed, an appreciation can be developed for the correlation between pressure and flowfield variables by comparing the extent of the separated region geometry as discussed previously and the size of the suction region. This correlation is shown in Fig. 11. The size of the suction region is observed to grow in an almost linear manner coinciding with the extent of the shear layer vortex.

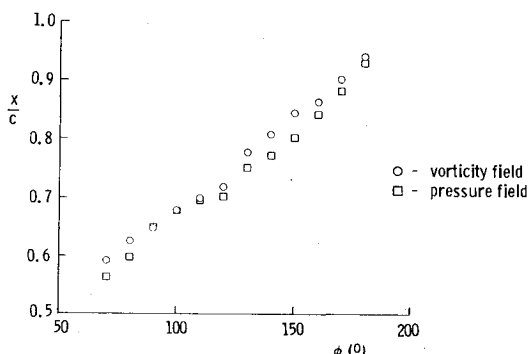


Fig. 11 Separated region length using vorticity and surface pressure distribution data, $Re = 410,000$, $k = 0.5$.

Conclusions

The unsteady, separated region generated over the upper surface of the airfoil by harmonic spoiler oscillations is identified as a dynamically evolving vortex-like structure bearing a strong resemblance to the one encountered in the dynamic stall flowfield. For high Reynolds number flow and dimensionless frequencies between zero and unity, the structure is observed to be attached to the spoiler (at least during the upstroke) and elongates primarily in the freestream direction. Its growth is observed to be directly proportional to time since formation and not closely correlated to the nonlinear spoiler motion.

The dimensionless characteristic growth rate of this vortex is observed to be directly proportional to the square root of the dimensionless frequency.

The primary source of vorticity following the structure's formation is the action of the accelerated freestream over the tip of the moving spoiler.

The geometric characteristics of the separation vortex are related to the extent of the suction region during the spoiler upstroke. The magnitude of the suction peak appears to be correlated with the laterally averaged vorticity distribution, and not with the maximum peak vorticity levels found in the shear layer. The vorticity field characterizing the outer shear layer and the corresponding surface pressure distribution were not closely correlated during the downstroke part of the cycle. The mechanisms which influence the behavior of the surface pressure distribution in these instances are believed to be related to flow conditions nearer the surface.

Acknowledgments

The research was sponsored by the Frank J. Seiler Research Laboratory (AFSC) under project/task 2307-F1. The authors gratefully acknowledge the efforts of C. Geddes, Instrument Maker, whose exceptional craftsmanship is responsible for the quality of the experimental apparatus. The Department of Aeronautics greatly assisted by providing the use of their wind-tunnel facility. Our thanks are also extended to D. Weiss for her painstaking efforts in the preparation of this manuscript.

References

- Viegas, J. R. and Coakley, T. J., "Numerical Investigation of Turbulence Models for Shock Separated Boundary-Layer Flows," AIAA Paper 77-44, Los Angeles, Calif., Jan. 1977.
- Trilling, L., "Oscillating Shock Boundary-Layer Interaction," *Journal of the Aeronautical Sciences*, Vol. 25, May 1958, pp. 301-304.
- Lighthill, M. J., "On the Weis-Fogh Mechanism of Lift Generation," *Journal of Fluid Mechanics*, Vol. 60, Pt. 1, 1973, pp. 1-17.
- Ham, N. D., "Aerodynamic Loading on a Two-Dimensional Airfoil during Dynamic Stall," *AIAA Journal*, Vol. 6, Oct. 1968, pp. 1927-1934.
- Crimi, P. and Reeves, B. L., "A Method for Analyzing Dynamic Stall," AIAA Paper 72-37, San Diego, Calif., Jan. 1972.
- Ericsson, L. E. and Reding, J. P., "Analytic Prediction of Dynamic Stall Characteristics," AIAA Paper 72-682, Boston, Mass., June 1972.
- McCroskey, W. J., Carr, L. W., and McAlister, K. W., "Dynamic Stall Experiments on Oscillating Airfoils," AIAA Paper 75-125, Pasadena, Calif., Jan. 1975.
- McAlister, K. W., Carr, L. W., and McCroskey, W. J., "Dynamic Stall Experiments on the NACA 0012 Airfoil," NASA Tech. Paper 1100, Jan. 1978.
- Mehta, U. B., "Dynamic Stall of an Oscillating Airfoil," AGARD Paper No. 23, Symposium on Unsteady Aerodynamics, Ottawa, Canada, Sept. 1977.
- McCroskey, W. J., "Some Current Research in Unsteady Fluid Dynamics," 1976 Freeman Scholar Lecture, *Transactions of the ASME, Journal of Fluids Engineering*, March 1977, pp. 8-39.
- McCroskey, W. J., "Introduction to Unsteady Aspects of Separation in Subsonic and Transonic Flow," AGARD Lecture Series No. 94, Three-Dimensional and Unsteady Separation at High Reynolds Numbers, Paper No. 6, Feb. 1978.

¹²Barnes, C. S., "A Developed Theory of Spoilers on Aerofoils," ARC Current Paper 887, July 1965.

¹³Barnes, C. S., "Two-Dimensional Normal Fences on a Flat Ridge," ARC Current Paper 863, Feb. 1965.

¹⁴Newman, B. G., "The Reattachment of a Turbulent Boundary-Layer Behind a Spoiler," Aeronautical Research Laboratories, Rept. A64, Melbourne, Australia, 1949.

¹⁵Lang, J. D., "The Dynamics of a Growing Separated Region on an Airfoil," Frank J. Seiler Research Laboratory Tech. Rept., SRL-TR-75-0005, Feb. 1975.

¹⁶Lang, J. D. and Francis, M. S., "Interaction of an Oscillating Control Surface with an Unsteady Separated Region," *Journal of Aircraft*, Vol. 13, Sept. 1976, pp. 687-694.

¹⁷Lang, J. D. and Francis, M. S., "Dynamic Loading on an Airfoil due to a Growing Separated Region," AGARD Symposium on Prediction of Aerodynamic Loading, Paper No. 26, NASA Ames Research Center, Calif., Sept. 1976.

¹⁸Keesee, J. E., Francis, M. S., and Lang, J. D., "A Technique for Vorticity Measurement in Unsteady Flow," AIAA Paper 78-801, San Diego, Calif., April 1978.

¹⁹Francis, M. S., Kennedy, D. A., and Butler, G. A., "Technique for the Measurement of Spatial Vorticity Distributions," *Review of Scientific Instruments*, Vol. 49, May 1978, pp. 617-623.

²⁰Francis, M. S., Lang, J. D., and Keesee, J. E., "Water Tunnel Measurements of Unsteady Separation," Frank J. Seiler Laboratory Tech. Rept. SRL-TR-78-0011, Dec. 1978.

From the AIAA Progress in Astronautics and Aeronautics Series..

AERODYNAMIC HEATING AND THERMAL PROTECTION SYSTEMS—v. 59 HEAT TRANSFER AND THERMAL CONTROL SYSTEMS—v. 60

Edited by Leroy S. Fletcher, University of Virginia

The science and technology of heat transfer constitute an established and well-formed discipline. Although one would expect relatively little change in the heat transfer field in view of its apparent maturity, it so happens that new developments are taking place rapidly in certain branches of heat transfer as a result of the demands of rocket and spacecraft design. The established "textbook" theories of radiation, convection, and conduction simply do not encompass the understanding required to deal with the advanced problems raised by rocket and spacecraft conditions. Moreover, research engineers concerned with such problems have discovered that it is necessary to clarify some fundamental processes in the physics of matter and radiation before acceptable technological solutions can be produced. As a result, these advanced topics in heat transfer have been given a new name in order to characterize both the fundamental science involved and the quantitative nature of the investigation. The name is Thermophysics. Any heat transfer engineer who wishes to be able to cope with advanced problems in heat transfer, in radiation, in convection, or in conduction, whether for spacecraft design or for any other technical purpose, must acquire some knowledge of this new field.

Volume 59 and Volume 60 of the Series offer a coordinated series of original papers representing some of the latest developments in the field. In Volume 59, the topics covered are 1) The Aerothermal Environment, particularly aerodynamic heating combined with radiation exchange and chemical reaction; 2) Plume Radiation, with special reference to the emissions characteristic of the jet components; and 3) Thermal Protection Systems, especially for intense heating conditions. Volume 60 is concerned with: 1) Heat Pipes, a widely used but rather intricate means for internal temperature control; 2) Heat Transfer, especially in complex situations; and 3) Thermal Control Systems, a description of sophisticated systems designed to control the flow of heat within a vehicle so as to maintain a specified temperature environment.

Volume 59—432 pp., 6 × 9, illus. \$20.00 Mem. \$35.00 List

Volume 60—398 pp., 6 × 9, illus. \$20.00 Mem. \$35.00 List

TO ORDER WRITE: Publications Dept., AIAA, 1290 Avenue of the Americas, New York, N.Y. 10019